View metadata, citation and similar papers at core.ac.uk

brought to you by CORE

provided by Elsevier - Publisher Connector

Electrochemical Measurement of Lateral Diffusion Coefficients of Ubiquinones and Plastoquinones of Various Isoprenoid Chain Lengths Incorporated in Model Bilayers

Damien Marchal, Wilfrid Boireau, Jean Marc Laval, Jacques Moiroux, and Christian Bourdillon

Laboratoire de Technologie Enzymatique, Unité associée au CNRS No 6022, Université de Technologie de Compiègne, 60205 Compiègne Cedex, and Laboratoire d'Electrochimie Moléculaire, Unité associée au CNRS No 7591, Université de Paris 7-Denis Diderot, 75251 Paris Cedex 05, France

ABSTRACT The long-range diffusion coefficients of isoprenoid quinones in a model of lipid bilayer were determined by a method avoiding fluorescent probe labeling of the molecules. The quinone electron carriers were incorporated in supported dimyristoylphosphatidylcholine layers at physiological molar fractions (<3 mol%). The elaborate bilayer template contained a built-in gold electrode at which the redox molecules solubilized in the bilayer were reduced or oxidized. The lateral diffusion coefficient of a natural quinone like UQ_{10} or PQ_9 was $2.0 \pm 0.4 \times 10^{-8}$ cm^2 s^{-1} at 30°C, two to three times smaller than the diffusion coefficient of a lipid analog in the same artificial bilayer. The lateral mobilities of the oxidized or reduced forms could be determined separately and were found to be identical in the 4–13 pH range. For a series of isoprenoid quinones, UQ_2 or PQ_2 to UQ_{10}, the diffusion coefficient exhibited a marked dependence on the length of the isoprenoid chain. The data fit very well the quantitative behavior predicted by a continuum fluid model in which the isoprenoid chains are taken as rigid particles moving in the less viscous part of the bilayer and rubbing against the more viscous layers of lipid heads. The present study supports the concept of a homogeneous pool of quinone located in the less viscous region of the bilayer.

INTRODUCTION

The two-dimensional mobility of electron carriers plays a central role in the respiratory and photoredox chains of bacteria, mitochondria, and chloroplasts (Mitchell and Moyle, 1985; Hauska and Hurt, 1982). Among these carriers, the isoprenoid quinones exhibit specific two-dimensional behaviors due to their high hydrophobicity. Natural ubiquinone (UQ_n, where n is the number of isoprenoid groups) and plastoquinone (PQ_n) molecules are only soluble in the inner part of the bilayer, and their lateral mobility is undoubtedly controlled by numerous parameters such as the conformation and the location of the molecules, the physical state of the quinone pool, the local lipid fluidity, and the protein crowding of the bilayer. Yet the influence of these parameters is not clearly characterized and is most often a matter of speculative discussion.

Several techniques have been developed to measure lateral diffusion coefficients of lipids in natural or artificial bilayers (for reviews see: Gennis, 1989; Tocanne et al., 1994). However, there is still much controversy on the order of magnitude of the diffusion coefficients of isoprenoid quinones, even when measured in simplified models like vesicles. The use of fluorescent quenching led to data in the ranges of 2×10^{-7} to 10^{-6} cm^2 s^{-1} (Fato et al., 1985, 1986; Lenaz et al., 1992) or $1–3 \times 10^{-7}$ cm^2 s^{-1} (Blackwell et al., 1987; Blackwell and Whitmarsh, 1990). In contrast, the diffusion coefficients determined by fluorescence recovery after photobleaching (FRAP) were found, for vesicles, in the 10^{-8} to 5×10^{-8} cm^2 s^{-1} range (Gupte et al., 1984; Chazotte and Hackenbrock, 1989; Rajarathnam et al., 1989; Chazotte et al., 1991).

Short-range diffusion coefficients are measured by fluorescence quenching. The main advantage of the technique consists of the use of unmodified quinones, because the oxidized form of the quinone directly quenches the fluorescent probes introduced into the bilayer (Fato et al., 1986). However, the diffusion-controlled dynamic quenching in membranes cannot be correctly described by the isotropic and three-dimensional theory of Stern-Volmer. Then the diffusion coefficients thus determined are often overestimated by one or two orders of magnitude, as already pointed out (Blackwell et al., 1987; Blackwell and Whitmarsh, 1990). The FRAP approach gives access to long-range diffusion coefficients that are judged to be more realistic in terms of electron transfer reactivities between redox partners of electrons chains (Chazotte and Hackenbrock, 1988; Chazotte et al., 1991). The technique is based on the dissipation of a gradient of bleached fluorescent dye molecules from a small photobleached spot or the diffusion of unbleached fluorescent dye molecules into a small photobleached spot, and it requires fluorescence labeling of the diffusing molecules. In general, the quinones themselves are labeled directly (Q_0C_{10}NBDHA in Gupte et al., 1984, or NBDUQ in Rajarathnam et al., 1989, where NBDHA = *N*-4-nitrobenzo-2-oxa-1,3-diazole-hexanoic acid and NBDUQ = 4-(*N*-(acetoxyethyl)-*N*-methyl-amino)-7-nitro-2,1,3-benzoxadiazole-UQ_{10}), but in some cases the fluorescent dye is only a model molecule solubilized in the bilayer (Chazotte

Received for publication 26 August 1997 and in final form 24 December 1997.

Address reprint requests to Dr. Christian Bourdillon, Laboratoire de Technologie Enzymatique, UPRES-A 6022 du CNRS, Université de Technologie de Compiègne, BP 529, 60205 Compiègne Cedex, France. Tel.: 33-03-44234405; Fax: 33-03-44203910; E-mail: christian.bourdillon@utc.fr.

© 1998 by the Biophysical Society

0006-3495/98/04/1937/12 $2.00

and Hackenbrock, 1989). This explains why the lateral diffusion coefficient of UQ_{10} has most often been found to be similar to the diffusion coefficient of the phospholipid in which it resided (Chazotte and Hackenbrock, 1989). Actually, the labeling of the natural quinone can be quite a drawback, because the relative change in the molecular weight, the polarity, and the conformation induced by grafted fluorescent labels can be substantial. Both the location and the lateral mobility of the molecule may be affected significantly.

A new electrochemical method of investigation of the mobility of redox carriers in artificial membrane systems has been developed recently (Torchut et al., 1994; Marchal et al., 1997). It consists of detecting the isoprenoid quinone by taking advantage of its redox reactivity. The need to graft a fluorescent label is thus avoided. The excitation and measurement technique is a chronocoulometry carried out at a judiciously chosen potential, which provides a means of quantitative analysis of the dissipation of the gradient of oxidized or reduced molecules from the electrode, which acts as a control point. Long-range lateral diffusion coefficients can then be determined, the long range being on the order of a few microns, as defined by Chazotte et al. (1991).

Electrochemical methods are very well suited for the study of electron carriers in general, and chronocoulometry is a technique of reference for the measurement of diffusion coefficients in solution (Bard and Faulkner, 1980). In the case of hydrophobic molecules like ubiquinones, the location of the redox head inside the lipid bilayer is a difficult constraint, because the working electrode has to be in contact with the hydrophobic part of the bilayer. The contact cannot be achieved in the spherical geometry of vesicles, but a new technology has been developed for supported bilayers (Miller and Majda, 1986; Torchut et al., 1994). The key point consists of the use of an array of cylindrical pores that are oriented perpendicularly to the electrode surface. These pores act as a template (Fig. 1) for the bilayer produced by self-assembly, according to the methods originally described for glass templates by Brian and McConnell (1984) and Kalb et al. (1992). It has been demonstrated recently that quantitative incorporation of ubiquinone and plastoquinone species in the artificial structure can be achieved through direct fusion of phospholipid vesicles to the hydrophobic first layer (Marchal et al., 1997).

The present paper describes a two-dimensional chronocoulometric study of various hydrophobic quinones incorporated at a physiological concentration level in a model membrane system. First of all, the making of the microporous electrode on the one hand, and the electrochemical analysis on the other hand, were refined so as to improve the sensitivity of the method to detect very low amounts of redox molecules incorporated into the bilayer. The diffusion coefficients of a set of ubiquinones and plastoquinones of different chain lengths were measured without any labeling of the molecules. The data provide a basis for a sound discussion of both the location and mechanism of lateral motion of long-chain isoprenoid quinones in the model layer.

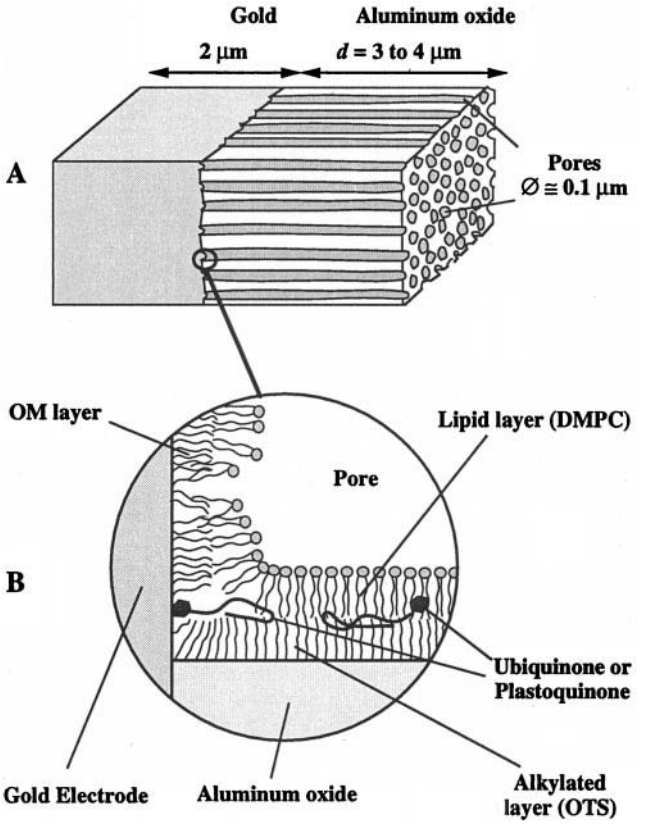

FIGURE 1 (*A*) General structure of the microporous electrode made of a porous aluminum oxide film attached to a gold electrode. The DMPC and isoprenoid quinone molecules are laterally mobile along the pore walls. (*B*) Enlarged schematic view of the bottom of a pore at the level of the gold/aluminum oxide interface. The alkylated/lipid bilayer is assembled on the inner surface of the porous aluminum oxide film. The octadecyl mercaptan (OM) treatment partially blocks the gold electrode. Despite the fact that the actual gold surface area is unknown, the pores area/gold area ratio is very high, at least 50 for an oxide thickness of 3.5 μm.

MATERIALS AND METHODS

Reagents

L-α-Dimyristoyl phosphatidylcholine (DMPC) (synthetics > 99% pure) was purchased from Sigma (St. Quentin Fallavier, France). UQ_{10}, UQ_6, UQ_2, PQ_2, and PQ_9 were from Sigma. UQ_8, UQ_5, UQ_4, and UQ_3 were a kind gift from EISAI Company (Tokyo). Octadecyltrichlorosilane (OTS) (Aldrich, Strasbourg, France) was vacuum distilled before use. Hexadecane (Aldrich) was dried over desiccated molecular sieves. Octadecyl mercaptan (OM) (Aldrich) was recrystallized in ethanol before use. Aluminum foil, 1 mm thick (Al 99.95%), was from Merck (Darmstadt, Germany). Organic solvents were high-performance liquid chromatography grade. Water with a typical resistivity of 18 MΩ was produced from Milli-Q purification system (Millipore, Les Ulis, France). All other chemicals were reagent grade.

Preparation of the OTS-treated oxides and aluminum oxide-coated gold electrodes

The modified electrodes were prepared with very thin aluminum oxide films (a few μm) produced in the laboratory. The procedure was first

described by Miller and Majda (1986) and modified by Parpaleix et al. (1992). Briefly, aluminum oxide films were generated by anodization of aluminum foils. The separation of the oxide film from the aluminum substrate and the removal of the barrier layer were performed by the method of Parpaleix et al. (1992). The thickness, *d*, of these films was between 3 and 4 μm and was routinely measured with an uncertainty of 10% by scanning electron microscopy. After rinsing and drying, the oxide films were alkylated into a freshly prepared OTS solution in hexadecane (1%, v/v). After a 10-min self-assembly, they were rinsed extensively with toluene and used immediately. They were transferred into a vacuum deposition apparatus (Edwards model E306A), where they were coated with ~2-μm-thick gold films. Finally, the gold-coated oxide films were mounted on the tip of a glass tube (3 mm in diameter) by the method of Miller and Majda (1986). The actual surface area of the pores was deduced from scanning electron microphotography (SEM) at a magnification of 20,000×. The actual surface area/apparent surface area ratio was 50 ± 8. Taking into account the pore's geometry and the geometrical surface area of the electrode tip (0.07 cm^2), the bilayer surface area was 3.7 ± 0.7 cm^2 for a 3.5-μm-thick oxide film. The final quality of the microporous electrodes was routinely controlled by the method of Marchal et al. (1997).

The self-assembly of OM on the remaining bare surface of gold, which brings about a substantial decrease in the level of the background current, was adapted from Bain et al. (1989). The microporous electrodes were dipped for 3 min in a 1 mM solution of OM in ethanol/water (4/1, v/v). Before use the electrodes were rinsed with ethanol and toluene to remove all unbound OM molecules, then with methanol, and finally with phosphate buffer.

Supported monolayer assemblies

Phospholipid vesicles were prepared from dried lipids as follows. A known amount of DMPC (~2.3 mg) was resuspended from the walls of a glass tube by vigorous vortexing in 5 ml of water. This solution was sonicated to clarity, four times for 3 min each with a Branson model 250 sonicator (Danbury, CT) set at 60 W power, the temperature being maintained between 40°C and 50°C, with a cold bath available, if needed. This stock solution was cleaned of titanium particles by centrifugation at 3000 × *g* and used for dilutions during the day. The mixed vesicles of DMPC and quinone were prepared at a quinone mole fraction twofold greater than the one expected in the bilayer (see Results and Discussion). The chloroform solution of DMPC and UQ_n (or PQ_n), in the required ratio, was evaporated under nitrogen flow and dried under vacuum for 1 h. DMPC and UQ_n (or PQ_n) were then resuspended and sonicated as above.

Direct fusion of unilamellar vesicles of lipids or mixed vesicles containing quinones on the inner surfaces of OTS-treated microporous aluminum oxide templates followed the procedure originally described for alkylated glass coverslips by Brian and McConnell (1984). The microporous electrodes were first wetted with methanol and rinsed with water in three different baths. The electrodes were then transferred and incubated for 30 min in the vesicles solution (7×10^{-4} M) for adsorption and fusion at 30°C. Before use, the oxides were extensively rinsed with water for at least 30 min to remove the adsorbed vesicles. It is worth emphasizing that the successive dippings of the electrode in the various solutions did not wash out the lipid layer. In contrast to the observed loss of the layer deposited on a planar surface (Brian and McConnell, 1984), the special geometry of the microporous template protects the structure when the tip of the electrode crosses the air/water interface.

Electrochemical measurements

An anaerobic electrochemical cell was fitted with three electrodes: a working microporous oxide film electrode, a KCl-saturated aqueous calomel reference electrode (SCE = 0.238 V versus the normal hydrogen electrode at 30°C), and a platinum foil auxiliary electrode. For measurements at different pH, the background solutions were prepared as follows: pH 4–7: 0.01 M citric acid/citrate buffers; pH 7–8: 0.01 M phosphate buffers; pH 8–11: 0.01 M carbonate buffers; pH 11–13: NaOH solutions. When necessary, the ionic strength was adjusted to 0.1 M with Na_2SO_4. Gentle bubbling of argon or nitrogen reduced the partial pressure of oxygen in the main compartment. The temperature was controlled at 30°C by water circulation in the outer jacket of the cell.

A PAR model 273 potentiostat controlled by a PC computer and a model 270 software package (EG&G Princeton Applied Research, Princeton, NJ) and a Voltalab 32 controlled by a PC computer and a Voltamaster software package (Tacussel, Radiometer Analytical, Villeurbanne, France) were used in parallel for cyclic voltammetry and chronocoulometry, respectively.

RESULTS AND DISCUSSION

The bilayer structure

It has recently been established that a structure similar to a bilayer can be elaborated through the direct fusion of phospholipid vesicles on the alkylated template of a microporous electrode (Marchal et al., 1997). In the present work, we proceeded similarly and built modified microporous electrodes exhibiting the following characteristic features.

The surface concentration of the monolayer of DMPC molecules was measured by the radiolabeling procedure described by Torchut et al. (1994), and found to be 250 ± 50 picomol cm^{-2}. At such a surface area per molecule (67 ± 13 $Å^2$ at 30°C), the monolayer behaves like a "liquid like" phase (Tscharner and McConnell, 1981). The fluidity of the structure is similar to that of a bilayer but, because the supporting layer is covalently bound to the aluminum oxide, only the upper lipid monolayer is capable of free lateral diffusion.

The fusion of DMPC vesicles containing a low molar fraction of isoprenoid quinones led to the quantitative incorporation of the hydrophobic quinone into the structure. The mass balances after fusion were checked out either spectrophotometrically after solvent extraction or routinely by coulometric measurements (Marchal et al., 1997). All of the incorporated quinone species can be reduced or oxidized at the built-in gold electrode. As expected, two electrons per quinone molecule were transferred in the electrochemical process whatever the pH. In agreement with the mechanism put forward by Kalb et al. (1992), the fusion of vesicles on the supporting layer results in our case to a twofold dilution of the quinone molar fraction. For example, fusion of vesicles at 2 mol% on the alkylated surface produces a quinone surface concentration close to $0.02 \times 250 \times 10^{-12} = 5 \times 10^{-12}$ mol cm^{-2}. It is equivalent to a quinone molar fraction of 1% in the unilamellar phospholipid vesicles used in FRAP techniques.

The stability of the bilayer supported on the microporous structure is sufficient to allow reproducible measurements over at least a day-long period. We chose to operate with quinones bearing at least two isoprenoid units. The water solubilities of the UQ_0 and UQ_1 are too high to ensure that they do not leak from the bilayer to the adjacent solution. To ascertain the stability and the solubility of the isoprenoid quinones in the bilayer, a microporous electrode was loaded in the presence of DMPC/quinone vesicles at equilibrium,

i.e., for ~2 h. After successive rinsing in NaOH (10^{-3} M) and in the buffer to remove all unfused vesicles, the amount of incorporated quinone was measured by cyclic voltammetry, by integration of the reduction peak recorded at a slow potential scan rate of 1 mV s^{-1}. The electrode was then submitted to a tentative quinone exchange. It was dipped in a solution of pure DMPC vesicles for 5 h. To pass from the inner part of the bilayer to the inner part of the vesicles, a minimum water solubility of the isoprenoid quinone is required. A new electrochemical determination of the quinone charge of the bilayer provided a measure of the quinone stability within the bilayer structure and an indication of its water solubility. Under such experimental conditions, the quinone charges remained unchanged in the cases of UQ_n or PQ_n, provided that $n \geq 3$. For UQ_2 and PQ_2, a small leakage was detected, clearly larger for the reduced forms (UQ_2H_2 or UQ_2H^-); nevertheless it occurred slowly enough (~2%/h) to be taken easily into account in the quantitative analyses of the experiments.

Chronocoulometric measurement of the lateral diffusion coefficient

As already pointed out, chronocoulometry is a reference method for the determination of diffusion coefficients of electrochemically active species in solution. The replenishment of electroactive molecules at the electrode/solution interface due to the diffusion of these molecules is monitored by the current resulting from the heterogeneous electron transfer taking place at this interface. The current versus time profile or the amount of electric charge transferred (integrated current) versus time profile gives insight into the dynamics of the diffusion layer. The method has been extended to the study of two-dimensional structures assembled either at the air-water interface (Charych et al., 1991) or in supported bilayers of electrochemically active amphiphiles (Miller et al., 1988; Torchut et al., 1994).

In the bilayer structure investigated here, the quinone molecules are laterally mobile and can reach the surface of the gold electrode by two-dimensional diffusion. Then the heterogeneous electron transfer can occur, provided that the electrode potential is conveniently settled. Similar to the first step of the FRAP experiments, which consists of fast photobleaching triggered by a laser pulse, the excitation step in chronocoulometry consists of a fast change (typical rise time 10 μs) of the electrode potential from an initial value at which the oxidized quinone is not reducible to a final value at which the electrochemical reduction is so rapid that it cannot be rate controlling compared to diffusion. The controlled potential is held at the latter value until the end of the measurement. The time dependence of the chronocoulometric charge q_{red}, i.e., the amount of electric charge transferred, is recorded during the "recovery" process, which is controlled by lateral diffusion. Fig. 2 gives an example of an experimental trace of the variation of q_{red} versus time t.

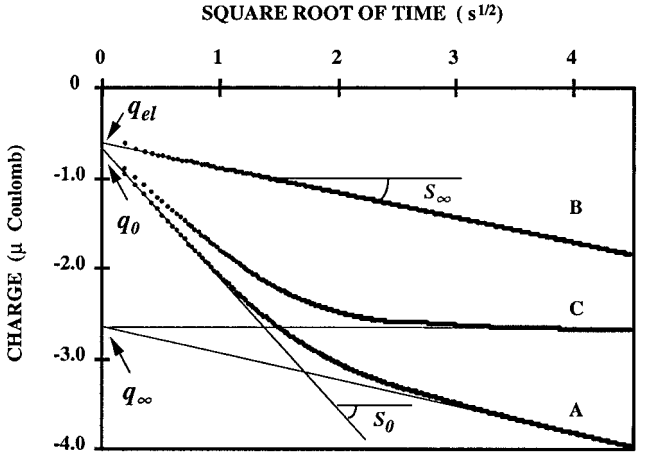

FIGURE 2 (*Curve A*) Typical chronocoulometric q versus $t^{1/2}$ plot recorded with a UQ_{10}-loaded microporous electrode. The equivalent UQ_{10} over DMPC molar ratio is 0.75%. The experiment was carried out, here for the oxidized molecule, at 30°C in 0.1 M phosphate buffer (pH 7). $E_1 = 400$ mV; $E_2 = -100$ mV; $E_3 = -700$ mV. The data sampling time was 50 ms. (*Curve B*) Background experimental trace. Same conditions as for curve A, in the absence of UQ_{10}. See text for the definitions of q_{el}, q_0, q_∞ and S_0, S_∞. (*Curve C*) Correction of curve A, which takes into account the contribution of the slope S_∞ measured for curve B. Curve C exhibits ideal behavior in the absence of background current. As d was 3.0 μm for this electrode, we found that $q_f = 1.8$ μC, $\Gamma_Q = 3.6$ picomol cm^{-2}, and $D_Q = 2.0 \times 10^{-8}$ cm^2 s^{-1}.

For microporous electrodes, q_{red} is proportional to $t^{1/2}$ at short times according to the following equation (Miller et al., 1988):

$$q_{red} = \frac{2q_f\sqrt{D_Q t}}{d\sqrt{\pi}} \quad (1)$$

with

$$q_f = A_B n F \Gamma_Q \quad (2)$$

The electric charge q_{red} is expressed in coulombs and t in s, q_f is the charge corresponding to the exhaustive reduction of the total amount of oxidized quinone incorporated in the bilayer, D_Q is the lateral diffusion coefficient of the oxidized quinone (in cm^2 s^{-1}), d is the thickness (cm) of the porous oxide film (i.e., the length of the pores supporting the bilayer assemblies), n is the number of electrons transferred per electroactive molecule ($n = 2$), A_B is the surface area of the bilayer (cm^2), and Γ_Q is the surface concentration of the quinone in the bilayer (mol cm^{-2}).

The overall electrochemical reaction is

$$Q + 2e + 2H^+ \leftrightarrow QH_2$$

where Q, QH_2, QH^-, are general abbreviations, respectively for, oxidized quinones, neutral reduced quinones, and anionic reduced quinones. For pH > pK_a (12.5), QH_2 is deprotonated into the hydroquinone anion QH^- (Rich, 1984; Marchal et al., 1997).

Equation 1 applies only to semiinfinite diffusion (Miller et al., 1988). To fulfill the condition, the time window of

measurement must not exceed a few seconds for a diffusion coefficient close to 10^{-8} cm^2 s^{-1} and a pore length d of ~3 μm. The curvature of the plot observed at longer times stems from the fact that the number of quinones in the porous structure is limited, and finally, all of the quinone pool is reduced in ~10–20 s. The total charge q_f measured at the plateau (curve C) can be used for the determination of the total amount of quinone incorporated in the structure.

The electrode potential can also be set initially at a value negative enough to provoke the two-electron reduction of Q into QH_2 or QH^-, depending on pH, for a delay long enough to ensure that the reduction is exhaustive. Then, in a chronocoulometric experiment symmetrical to the one described above, the excitation potential step can be chosen so that the chronocoulometric q_{ox} versus t curve reflects the oxidation of QH_2 or QH^- back to the oxidized quinone Q, and

$$q_{ox} = \frac{2q_f\sqrt{D_{QH2}t}}{d\sqrt{\pi}} \quad (3)$$

D_{QH2} (or D_{QH^-}, depending on pH) is the lateral diffusion coefficient of the reduced quinone. Obviously q_f has the same value in Eqs. 1 and 3. An interesting consequence is that the lateral diffusion coefficients of the oxidized and reduced forms of the quinone can be determined independently.

The existence of a background current disturbs the theoretical behavior. Three additional experimental parameters must be taken into account to extract the current, which can be quantitatively analyzed according to the theoretical treatment summarized above. As illustrated in Fig. 2, q_{el} is the charge of the electrode double-layer interface, and S_∞ is the slope of the integrated background current versus time linear dependence. These two parameters were measured in the absence of incorporated quinone. The sensitivity of the method was markedly affected by their absolute values, because they enhanced the noise in the signal-to-noise ratio. We succeeded in reducing their levels by proceeding as detailed below. The last additional parameter, $q_0 - q_{el}$, is the electric charge originating in the adsorption of quinone on the gold electrode surface. The very small amount of adsorbed quinone (typically 3×10^{-13} mol/electrode, i.e., an electric charge of 0.06 μC) was not counted in the pool of mobile quinone because the adsorbed species needed no diffusion to reach the electrode and reacted instantaneously. Finally, $q_f = q_\infty - q_{el} - (q_0 - q_{el}) = q_\infty - q_0$, and the background-corrected slope of the linear portion of the q versus $t^{1/2}$ plot is $S = S_0 - S_\infty$. Then according to Eq. 1,

$$D = \frac{\pi d^2}{4}\left(\frac{S_0 - S_\infty}{q_\infty - q_0}\right)^2 \quad (4)$$

The actual surface area of the gold electrode need not be known for the calculation of the lateral diffusion coefficient, D, D being equal to D_Q (when the sign of the potential step is such that an electrochemical reduction takes place) or to D_{QH2} or D_{QH^-} (in the opposite case). The accuracy of D is mainly related to the accuracy of d. As explained in Materials and Methods, d is given by SEM measurement of the thickness of the oxide layer with a relative uncertainty of 10%. The sensitivity of the method is experimentally limited at low quinone charges by the values of q_{el} and S_∞, the electrode background parameters. It is well documented that a bare gold electrode is very prone to oxidation at potentials higher than 0.2 V/SCE, the metal being oxidized in various species, the nature of which depends on pH and electrolyte composition (recently reviewed in Burke et al., 1994). The net result is a large increase in both q_{el} and S_∞, and the emergence of at least one faradaic peak at about −0.1 V/SCE (pH 7), corresponding to the reduction of the gold oxides. In particular, the presence of chloride anions must be carefully avoided, and we had to minimize the introduction of Cl^- resulting from the use of a KCl-saturated aqueous calomel reference electrode, a very small leakage of KCl from the junction of the reference electrode being unavoidable.

To improve the signal-to-background ratio, we developed two strategies. The first consisted of fine-tuning the potentials at which the gold electrode was stepped and the accompanying delay times needed to reach a steady state before chronocoulometric data acquisition. The insert in Fig. 3 shows the locations, in the cyclic voltammogram, of the three potentials E_1, E_2, and E_3, successively applied. Each was settled, at each pH, according to the following constraints. For a chronocoulometric reduction, E_1 must be chosen positive enough to ascertain exhaustive oxidation of the quinone species with minimum gold oxidation. Accordingly, at pH 7, the electrode was poised at +400 mV/SCE for 100 s. The gold oxides, produced at 400 mV, were

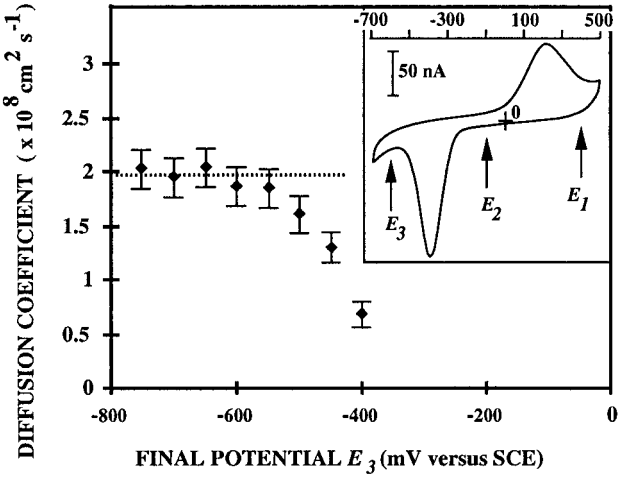

FIGURE 3 Experimental determination of potential E_3 for the final chronocoulometric step. The lateral diffusion coefficient of UQ_{10} was correctly determined at this pH for $E_3 \leq -600$ mV/SCE. The experiments were carried out at pH 7 in 0.1 M phosphate buffer, 30°C. The equivalent molar fraction of the quinone pool was 0.8%, with a total charge of 1.9×10^{-6} C per microporous electrode (9.8 picomol UQ_{10}). (*Insert*) Cyclic voltammogram at a potential scan rate of 10 mV s^{-1}. The arrows indicate the locations of potentials E_1 to E_3 for the chronocoulometric steps. The shape of the voltammogram was previously discussed (Marchal et al., 1997).

reduced in 30 s at the intermediate potential E_2, which was taken as close as possible to the foot of the quinone reduction peak, $E_2 = -100$ mV/SCE at pH 7. The chronocoulometric measurement itself occurred at the final potential E_3, which must be negative enough to ensure that the process was diffusion controlled. Fig. 3 demonstrates that such a condition was fulfilled provided that $E_3 \leq -600$ mV/SCE, at pH 7, because the value of the diffusion coefficient thus determined was then E_3 independent. The three potentials E_1, E_2, and E_3 were tuned at each pH, either for the measurement of D_Q with a negative $E_2 - E_3$ potential step, or for the measurement of D_{QH2} (or D_{QH2}) with a positive $E_2 - E_3$ potential step.

The aim of the second strategy was the modification of the gold interface so as to decrease the charge of the gold electrode double-layer interface by partially blocking the electrode surface. The strong adsorption of *n*-alkyl thiol monolayers on gold has been used in numerous works as a rational approach for the elaboration of interfaces with well-defined structures (Bain et al., 1989). It was recognized early on that gold electrodes covered with adsorbed alkyl monolayer exhibited low background currents (Porter et al., 1987), but their use was limited because of the risk of partial or even complete inhibition of the heterogeneous electron transfer (Bilewicz and Majda, 1991). We reached a compromise consisting of dipping the unloaded microporous electrodes in a 1 mM alcoholic solution of OM for 3 min. The resulting improvement was very satisfactory, because the background noises, both q_{el} and S_∞, were reduced ~10 times. A longer treatment with the OM solution (for example, 15 min) led to a further background decrease, but the appearance of overpotentials in the voltammogram of UQ_{10} revealed unwanted inhibition of the heterogeneous electron transfer. Fine-tuning of the potential steps and OM treatment enabled us to achieve the chronocoulometric determination of lateral diffusion coefficients in the range of 2×10^{-9} to 10^{-7} cm^2 s^{-1} for microporous electrode loads of 0.2 mol% quinone.

Lateral diffusion coefficient of UQ_{10} in the model bilayers

The chronocoulometric method was used extensively to measure the lateral diffusion coefficient of UQ_{10} in various experimental situations.

The first parameter studied was the effect of the quinone loading level. Under certain conditions it has been claimed that nonphysiological concentrations of ubiquinone tend to form separate phases (Stidham et al., 1984; Cornell et al., 1987; Castresana et al., 1992). The direct measurement of the dependence of the diffusion coefficient of UQ_{10} on the UQ_{10} concentration could help answer this question. Therefore a set of microporous electrodes was loaded with DMPC vesicles containing various UQ_{10} concentrations. The fusion gave reliable and reproducible results up to 3 mol% final equivalent quinone molar fractions. Reproducible loadings and behaviors with higher molar fractions could not be obtained. The maximum stable concentration of UQ_{10} in the interlayer of both vesicles and supported layers is probably related to the large size of the ubiquinone molecule. For example, if the UQ_{10} molecule is assimilated to a disk ~3 nm in diameter (see Table 1 and Discussion), positioned parallel to the membrane midplane, ~50% of the interlayer area is occupied by ubiquinone molecules at a UQ_{10} molar fraction of only 5 mol% (12.5 picomol UQ_{10}/cm^2 for 2×250 picomol phospholipid/cm^2). Then the interlayer becomes overcrowded. Such a rough but simple model helps in understanding why only experiments performed at physiological isoprenoid quinone concentrations (less than 3 mol%) are relevant, as has already been pointed out by several authors (see, for example, Chazotte et al., 1991; Handa et al., 1991; Metz et al., 1995).

Fig. 4 shows that the lateral diffusion coefficient in the supported bilayer is independent of the UQ_{10} molar fraction over a 15-fold range from 0.2 to 3 mol%. As the electrochemical technique involves all of the UQ_{10} molecules reaching the electrode surface, and not simply labeled ones, which might be affected by the presence of the label, the result rules out any partition of the quinone molecules in domains allowing different mobilities in such a model of membrane. It also rules out a significant contribution of electron hopping between immobile UQ_{10} molecules to the measured electric current, because the apparent diffusion coefficient would then be strongly concentration dependent (Charych et al., 1991).

The temperature dependence of the lateral mobility of UQ_{10} was investigated between 15°C and 40°C. Arrhenius plots (not shown) were linear and monophasic over the explored temperature range, and the apparent activation energy for the diffusion step was 13 ± 2 kcal mol^{-1}. This temperature dependence is similar to that reported for the mobility of ubiquinone by Chazotte and Hackenbrock

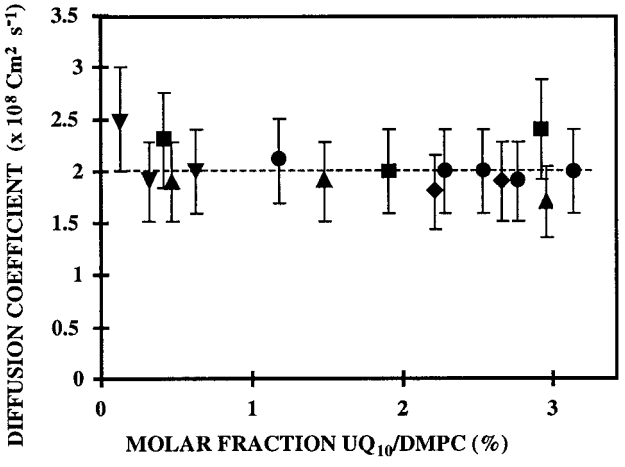

FIGURE 4 Variation of the lateral diffusion coefficient of UQ_{10} in the model bilayer with the equivalent quinone molar fraction. Chronocoulometry at 30°C. ◆, ▼, ■, ▲, ●, Five microporous electrodes loaded successively with various quinone molar fractions.

TABLE 1 Lateral diffusion coefficients of isoprenic quinones in supported lipid layers

Isoprenic quinones	N (carbon bonds in the chain)	$\bar{a}$* (nm)	Lateral diffusion coefficient: Calculated# ($\times 10^8$ cm^2 s^{-1})	Lateral diffusion coefficient: Measured§ ($\times 10^8$ cm^2 s^{-1})
UQ_2 and PQ_2	8	0.64	4.56	4.6 and 5.2 ± 1
UQ_3	12	0.78	3.72	4.4 ± 0.9
UQ_4	16	0.90	3.23	3.6 ± 0.8
UQ_5	20	1.00	2.89	3.0 ± 0.6
UQ_6	24	1.10	2.63	2.6 ± 0.5
UQ_8	32	1.27	2.28	2.3 ± 0.5
PQ_9	36	1.35	2.15	2.3 ± 0.5
UQ_{10}	40	1.42	2.04	2.0 ± 0.4

Comparison at 30°C between experimental results and a calculation using a continuum fluid hydrodynamic model.

*Mean radius of the model cylinder calculated from Eq. 5.

#Calculated from Eq. 6 with $\eta = 0.9$ poise.

§Chronocoulometric measurements on microporous electrodes.

(1989), who used FRAP measurements on phospholipid-enriched mitochondrial membranes. The lack of phase transition, at ~24°C, for the supported DMPC layers is due to lipid-OTS interactions in the midplane of the bilayer, as has been already explained (Tscharner and McConnell, 1981; Torchut et al., 1994). It is also worth emphasizing that the ubiquinone loading charges of the microporous electrodes were not affected by the temperature changes, an observation underscoring again that UQ_{10} was completely miscible in the artificial bilayer in the concentration range studied.

The influence of pH on the lateral mobility of UQ_{10} was investigated at last. The use of microporous electrodes provides a means of direct electrochemical study of totally water-insoluble quinones in an aqueous environment containing a pH buffer. The pK_a of the following acid/base equilibrium:

$$UQH_2 \leftrightarrow UQH^- + H^+$$

being 12.5 (Rich, 1984; Marchal et al., 1997), three species, UQ_{10}, $UQ_{10}H_2$, and $UQ_{10}H^-$, are involved. The electrochemical behavior of the quinone differs in the two pH ranges, because the electrochemical reversibility can be reached only at high pH (Gordillo and Schiffrin, 1994; Marchal et al., 1997). The study of the lateral mobility over a large pH range may help to determine if the mobility, and maybe the location, of the ubiquinone in the supported bilayer is sensitive to the redox and acid/base states of its quinone head. Within experimental uncertainty, we found that the lateral diffusion coefficient of UQ_{10} was $2.0 \pm 0.5 \times 10^{-8}$ cm^2 s^{-1} (at 30°C), whatever the buffer and ionic strength (up to 0.5 M) in the 4–13.5 pH range. The reversibility of the electrochemical process at pH 13, observed in cyclic voltammetry (Marchal et al., 1997), allowed us to carry out the chronocoulometric measurement of the lateral diffusion coefficients of either UQ_{10} or $UQ_{10}H^-$ if the hydroquinol form is not protonated inside the bilayer, $UQ_{10}H^-$ being the predominant form of the reduced quinone when it comes in contact with the electrode at this pH (Marchal et al., 1997), or both UQ_{10} and $UQ_{10}H_2$ if the hydroquinol form is protonated inside the bilayer. In the presence of the pH 13 buffer, we also found $2.0 \pm 0.5 \times 10^{-8}$ cm^2 s^{-1} for the lateral diffusion coefficient of the reduced quinone. At lower pH, for example at pH 7, we measured a lateral diffusion coefficient of $1.7 \pm 0.5 \times 10^{-8}$ cm^2 s^{-1} for $UQ_{10}H_2$. Obviously the mobilities of both the oxidized and reduced forms of the quinone are identical within experimental uncertainty.

Influence of the length of the isoprenoid chain on the lateral diffusion coefficient

The ability to determine the lateral diffusion coefficients of molecules bearing no label offered an interesting opportunity for the study of the influence of the hydrophobic chain on the location and mobility of ubiquinone or plastoquinone molecules within bilayers. The lateral diffusion coefficients of nine isoprenoid quinones were then determined (Fig. 5). As can be seen in Fig. 5, the lateral mobility of the quinone molecules in the supported bilayer decreases significantly when the length of the hydrophobic isoprenoid tail increases. The diffusion coefficient of the short tailed quinones (UQ_2, UQ_3, and PQ_2) is close to the diffusion coefficient of DMPC measured in the same structure (5.0×10^{-8} cm^2 s^{-1} at 30°C, from Torchut et al., 1994). It decreases to 2.0×10^{-8} cm^2 s^{-1} for quinones of higher molecular weights (UQ_9, UQ_{10}, PQ_9).

The measurement of lateral diffusion coefficients of molecules incorporated into experimental models of bilayers and the elaboration of theoretical models that can justify the data are a matter of substantial disagreement in the literature. Only the "long-range" approaches will be considered

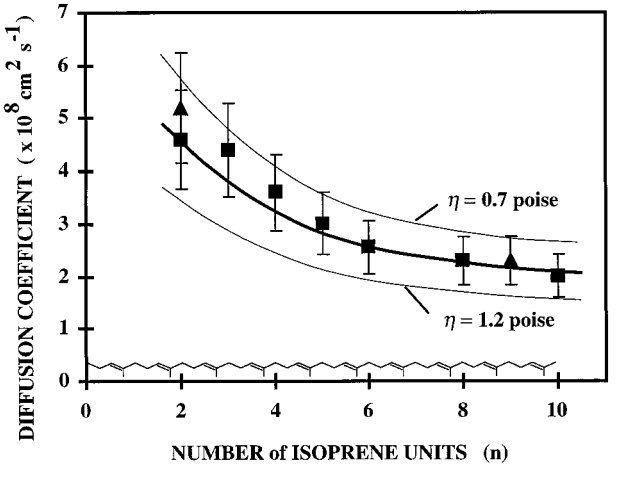

FIGURE 5 Variation of the lateral diffusion coefficient of UQ_n (■) and PQ_n (▲) with the number of isoprene units making the tail. Chronocoulometric measurements were made at 30°C with microporous electrodes loaded with quinone charges between 1 and 3 mol%. Each point represents the average of at least six measurements. The thick curve is computed according to Eq. 6, with $\eta = 0.9$ poise, and the thin curves with $\eta = 0.7$ poise and $\eta = 1.2$ poise.

here. The discussion related to the other approaches is also well documented (Rajarathnam et al., 1989; Tocanne et al., 1994; Metz et al., 1995). Essentially two "long-range" theoretical models have been put forward to justify the two types of experimental results obtained with model membrane systems: 1) The "free volume" model was formulated by Cohen and Turnbull (1959). It predicts that the lateral mobility of a species should not depend on its size. Labeled lipids (Vaz et al., 1985) or other labeled hydrophobic molecules (Rajarathnam et al., 1989; Balcom and Petersen, 1993) were found to behave accordingly. 2) The continuum fluid hydrodynamic model, interpreting the mobility in terms of Brownian motion of particles in a viscous medium, was initially proposed by Saffman and Delbrük (1975). It was successfully tested with proteins (Vaz et al., 1984) and, recently, with smaller molecules (Johnson et al., 1996).

The free volume model cannot be used to analyze quantitatively the diffusion of the isoprenoid quinones located inside the supported bilayer examined in the present work, because it predicts that the diffusion coefficients of rigid solute molecules that are comparable in size to the lipids are essentially constant and equal to the lipid diffusion coefficient, in contradiction to the experimental behavior we observed. Obviously such a model cannot justify the twofold increase that we found between the diffusion coefficients of UQ_6 and UQ_2 (see Fig. 5).

We propose a very simple approach within the framework of the continuum fluid hydrodynamic model, taking into account the adaptations that have already been put forward to apply the model to the studies of the lateral mobilities of lipids or integral proteins (Galla et al., 1979; Hughes et al., 1981; Vaz et al., 1985). One key point is that, in agreement with various groups (Ulrich et al., 1985; Rajarathnam et al., 1989; Chazotte et al., 1991; Metz et al., 1995), we assume that isoprenoid quinones are solubilized in the hydrophobic core of the bilayer. The first assumption of the model consists of locating the isoprenoid quinones in the midplane of the bilayer. According to recent molecular dynamics simulations of phospholipid bilayer/water systems (Bassolino-Klimas et al., 1993; Wilson and Pohorille, 1994; Pastor, 1994), the atomic density is lowered at the center of the bilayer, i.e., the density profile is complex compared to that of a uniform hydrocarbon phase. Consequently, the midplane appears to be the less crowded part of the structure. The local viscosity at midplane was evaluated to be much smaller than the viscosity in the polar head layers (Venable et al., 1993). We believe that the molecule of isoprenoid quinone occupies a rigid volume, the simplest form of which we can think of is a flat cylinder of radius a and height h, whose disk section is parallel to the bilayer midplane. This flat cylinder undergoes Brownian motion in the hydrophobic part of the bilayer (see Appendix). It is worth emphasizing that the cylinder height does not span the whole bilayer, as the proteins do in the model of Saffman and Delbrük (1975), because, in the present model, the upper limit of h is the thickness of the hydrophobic core of the bilayer (~3 nm).

To evaluate the equivalent radius a of the flat cylinder, we can proceed as follows. The isoprenoid chains being flexible (although it is known that the flexibility of *trans*-polyisoprene is restricted by hindered internal rotation), a statistical approach is the most appropriate for calculating the average size of the molecules. Conformational statistics of carbon chains is a well-known problem in macromolecular chemistry. Isoprenoid molecules were extensively studied earlier, because natural rubber and gutta percha are *cis* and *trans* isoprenoid polymers, respectively. Detailed calculations were reported by Volkenstein (1963) for *trans*-isoprenoid chains like those of UQ_n and PQ_n. The mean quadratic length $(2\bar{a})^2$ between the two tips of the carbon chain can be approximated by

$$(2\bar{a})^2 = 9Nl_c^2 \tag{5}$$

where N is the number of carbon bonds in the main chain (four for each isoprenoid unit), and l_c is the average length of one carbon-carbon bond in the main chain. The later has a value $l_c = 1.50$ Å, which is the average between three C—C simple bounds of 1.54 Å length and one C═C double bound of 1.35 Å. The mean radius of the cylinder is then taken as half the statistical length given by Eq. 5, i.e., $\bar{a} = 1.5l_c\sqrt{N}$. Despite the fact that the original calculation concerned an isoprenoid chain in a solvent, it seems reasonable to use here this evaluation, because the hydrophobic internal region of the bilayer is thicker, typically 3 nm (Gennis, 1989; Heller et al., 1993), than the diffusing molecule (see Table 1). Last, we assume that the quinone head introduces no significant increase in $\bar{a}$ because, as was recently demonstrated, the plane of the quinone ring would be preferentially oriented parallel to the lipid chain (Metz et al., 1995), i.e., parallel to the axis of the cylinder.

The exact hydrodynamic solution established for a similar model by Hughes et al. (1981) predicts limiting situations that correspond to the theoretical treatment of Saffman and Delbrück (1975) on the one side and an asymptotic behavior on the other. As detailed in the Appendix, the present case falls in line with the asymptotic behavior, and the lateral diffusion coefficient D is given by

$$D = kT/16a\eta_{head} \tag{6}$$

The viscosity η_{head} of the polar head region can be assimilated to the overall lipid viscosity because the contribution of the inner part of the bilayer to the overall viscosity is very low (Venable et al., 1993). At 30°C, η_{head} lies between 0.75 and 1.5 poise (Vaz et al., 1984, 1985).

Table 1 and Fig. 5 show that the simple model thus elaborated predicts with good accuracy both the absolute value of the diffusion coefficient and its dependence on the isoprenoid chain length. The best fit was obtained for $\eta_{head} = 0.9$ poise, a value very close to the viscosity evaluated at 30°C for model bilayers (Vaz et al., 1984, 1985).

CONCLUSION

The chronocoulometric technique described in the present paper provides a means of measurement of long-range lateral mobilities in bilayers, as well as the widely used FRAP technique. The former technique can be used only for the determination of diffusion coefficients of electrochemically active electron carriers. Its intrinsic advantage is the direct detection of the redox state of electron carrier molecules, which need not be additionally labeled. However, the technique relies upon the construction of a sophisticated electrochemical interface, and unfortunately, at this stage of development, it cannot be applied to the study of unsupported bilayers and living intact cells. The following discussion is thus restricted to artificial models of bilayers.

A few years ago, a controversy appeared in discussions dealing with the rate and regulation of energy transfer in respiratory chains. It concerned, in particular, the order of magnitude of the diffusion coefficients of isoprenoid quinones in artificial models of lipid bilayers such as vesicles. Data in the 10^{-7} to 10^{-6} cm^2 s^{-1} range were presented as the results of measurements of fluorescence quenching (Fato et al., 1985, 1986; Blackwell et al., 1987; Blackwell and Whitmarsh, 1990; Lenaz et al., 1992), whereas FRAP measurements gave 10^{-8} to 5×10^{-8} cm^2 s^{-1} (Gupte et al., 1984; Chazotte and Hackenbrock, 1989; Rajarathnam et al., 1989; Chazotte et al., 1991). Moreover, the latter authors emphasized that the isoprenoid quinones could not diffuse faster than the lipid. Our results confirm such a conclusion and the order of magnitude found by these authors for the diffusion coefficients of the isoprenoid quinones. However, another more or less explicit conclusion is also put forward in their papers: the rates of diffusion of the isoprenoid quinone and the lipid are similar. Taking such a conclusion as granted implies that the investigation of the influence of the length of the isoprenoid chain on the mobility of the electron carrier becomes pointless. It seems that our measurements give evidence of an actual dependence. Therefore, two questions arise: Is the use of supported bilayers relevant to the study of lateral diffusion of isoprenoid quinones in phospholipid bilayers? We are well aware that the main limitation of our experimental model of a supported bilayer is that only the upper layer is actually an autoassembled monolayer of lipids not attached to the support. The second question concerns the FRAP experiments: Does the diffusion of the ubiquinone analogs used correctly mimic that of unlabeled isoprenoid quinones, especially the ones which, like UQ_{10}, bear a long chain?

The answer to the first question is that, as shown in earlier studies, the lateral mobility of the upper lipid monolayer is not affected by the fact that the bilayer is supported (Tscharner and McConnell, 1981; Torchut et al., 1994). Furthermore, the FRAP and electrochemical measurements of the lipid mobility converge remarkably. For example, the FRAP technique gives a lateral diffusion coefficient of 5.0×10^{-8} cm^2 s^{-1} for DiI, a fluorescent lipid analog, in phospholipid vesicles at 30°C (Chazotte and Hackenbrock, 1989), and an identical value is found for a redox DMPC analog in the supported bilayer (Torchut et al., 1994). This indicates that there is no strong friction between the upper monolayer and the alkyl chains of the OTS layer linked to the support, i.e., that the individual layers of a bilayer are not strongly coupled, as far as hydrodynamics are concerned. This is also corroborated by molecular dynamics simulations, which predict a very low microviscosity at the center of the bilayer (Pastor, 1994). For the lateral motion of isoprenoid quinones, we cannot exclude the possibility that the friction between the attached OTS layer and the quinone may be stronger than in unsupported bilayers. The lateral diffusion coefficient of the quinone may be lowered in consequence, but the phenomenon cannot justify the significant dependence on the length of the isoprenoid chain reported in Fig. 5.

Considering, then, the second question, it is worth emphasizing that any grafting of a molecule with a probe may affect altogether its size, its conformation, and its interactions with the bilayer. In FRAP experiments the probes are fluorescent dyes, which may render the quinone analog (for instance, the NBDHA derivative) more hydrophilic than the native ubiquinones or plastoquinones. Then the location and even the mechanism of lateral diffusion of the labeled molecule in the bilayer can be dramatically altered. This is especially true for the short-chain ubiquinone analog Q_oC_{10}NBDHA used by Gupte et al. (1984) and Chazotte et al. (1991), and this may be the reason why its lateral diffusion coefficient of 4.9×10^{-8} cm^2 s^{-1} at 30°C is similar to that of the labeled phospholipid. A more realistic analog, NBDUQ, was synthesized by Rajarathnam et al. (1989). However, it was incorporated at relatively high final concentrations, i.e., between 2 and 6 mol% with respect to lipids, and there remained a doubt about its exact location in the bilayer compared to that of native UQ_{10}. That may explain why the diffusion coefficients of both the labeled lipid and isoprenoid quinone then fell to 1.3 and 1.1×10^{-8} cm^2 s^{-1}, respectively. Furthermore, it appears that no unified investigation of the dependence of the quinone mobility on the length of its isoprenoid chain has been carried out by means of the FRAP technique.

The systematic study of the influence of the isoprenoid chain length reported here, going from UQ_2 and PQ_2 to PQ_9 and UQ_{10}, may help in getting new insight into the location of ubiquinone or plastoquinone within the lipid bilayer. The lateral diffusion coefficients we determined correlate very well with the hydrodynamic volumes of the isoprenoid quinones, and both their absolute values and chain length dependencies can be quantitatively analyzed in the framework of the continuum fluid hydrodynamic model. Such a result strongly supports the concepts of several authors (Ulrich et al., 1985; Chazotte and Hackenbrock, 1989; Rajarathnam et al., 1989; Metz et al., 1995), who believe that the natural quinones move within the hydrophobic part of the bilayer.

At the present stage we suggest that state-of-the-art knowledge concerning the location and the movement of

natural quinones UQ_n and PQ_n in lipid bilayers could be formulated as follows. The quinone is located in the less crowded part of the bilayer, in the vicinity of the midplane. The local viscosity being rather low, the quinone mobility is more likely controlled by the drags of the top and bottom of the molecule than by the local viscosity of the medium. This is in agreement with previous evidence of the existence of a fluidity gradient detected by nuclear magnetic resonance across a membrane (Seelig and Seelig, 1980), and with the results of molecular dynamics simulations applied to the diffusion of a small molecule like benzene in a DMPC bilayer (Bassolino-Klimas et al., 1993). In the latter study it was concluded that the rate of lateral diffusion of benzene should depend on its location within the bilayer and should be faster in the midplane vicinity than near the polar heads. The equivalent radii of UQ_{10} and PQ_9 being much larger than those of UQ_2 or PQ_2 (1.4 versus 0.64 nm; see Table 1), the bigger the molecule, the harder it rubs against the relatively more viscous layers of polar heads and the slower the mobility. This is also consistent with the kinetic results obtained for transbilayer electron transfer rates (Ulrich et al., 1985). The longer the isoprenoid chain, the slower the electron transfer rate, or in other words, the higher the hydrophobicity, the more difficult the access of the quinone head to the polar region.

In our quantitative treatment, the solid shape ascribed to the isoprenoid quinone to model its statistical size is not crucial. We considered a flat cylinder. A change in the geometrical shape would affect the absolute value of the diffusion coefficient calculated according to the Stokes-Einstein equation; nevertheless, the variation with the chain length would remain quite similar. Another point worth mentioning concerns the lateral mobilities of the oxidized and reduced forms of the quinones. At pH 13, we found identical diffusion coefficients for the oxidized and reduced forms. We know that the reduced quinone could be ionized at this pH, because the pK_a of the first deprotonation of UQ_nH_2 is 12.5 (Marchal et al., 1997); thus it may exist in the bilayer either in its neutral UQ_nH_2 or in its negatively charged form UQ_nH^-. Because of its charge, the latter is the most prone to undergoing a change of location inside the lipid bilayer. The absence of change in the experimentally determined lateral diffusion coefficient after reduction and possible deprotonation indicates that this is quite unlikely. The reduced and oxidized quinones behave similarly in the lipid bilayer. The independence of the lateral diffusion coefficient on the redox state of the quinone was also experimentally observed in earlier studies measuring the quenching of steady-state fluorescence of natural quinones (Blackwell et al., 1987), although the order of magnitude of the measured diffusion coefficients was then markedly different (2×10^{-7} cm^2 s^{-1}).

In the experimental model of supported membrane elaborated in the present work, we found, for both UQ_{10} and PQ_9, a lateral diffusion coefficient two to three times smaller than the lateral diffusion coefficient of DMPC. The hydrodynamic model used to justify the data, and the data themselves, are consistent with a homogeneous pool of quinones located and moving in the less viscous region of the bilayer (Chazotte and Hackenbrock, 1989; Chazotte et al., 1991). They rule out the sometimes evoked possibility of a partition of the quinone population (Millner and Barber, 1984; Fato et al., 1985; Lenaz et al., 1992); one part is located in the region of low viscosity of the bilayer and thus is rather mobile, with diffusion coefficients of 10^{-6} to 10^{-7} cm^2 s^{-1}.

APPENDIX: DRAG COEFFICIENT OF A CYLINDER MOVING ALONG THE CORE OF A BILAYER

Hydrodynamic approaches of the problem were previously presented to model the lateral mobility of membrane components (Saffman and Delbrück, 1975, and Hughes et al., 1981). In the present case it is essential to keep in mind that the movement of the cylinder takes place within the less viscous part of the model bilayer.

We consider the Brownian motion of flat cylinders (radius a, height h), representing ubiquinone molecules, in an interlayer of low viscosity ($\eta_{midplane}$) located between two markedly more viscous layers, in such a way that the top and the bottom of each cylinder rub these more viscous layers. The upper layer is made of the phospholipid polar heads; the lower layer is made of the immobilized heads of the OTS layer. For the sake of simplicity and because the viscosity of the lower OTS layer is not known, we assume that the two extreme layers exert the same viscous effect (viscosity = η_{head}) on the two parts, top and bottom, of the cylinder. According to Hughes et al. (1981), the system is characterized by the following dimensionless parameter:

$$\epsilon = a(\eta_{head} + \eta_{head})/h\eta_{midplane} = 2a\eta_{head}/h\eta_{midplane}$$

The diffusion coefficient is related to the drag coefficient λ by the Einstein relation:

$$D = kT/\lambda$$

The exact solution for the computation of λ, whatever the value of ϵ, was given by Hughes et al. (1981):

$$\lambda = 4\pi(\eta_{head} + \eta_{head})a\Lambda(\epsilon) = 8\pi\eta_{head}a\Lambda(\epsilon)$$

where $\Lambda(\epsilon)$ is the reduced drag coefficient.

Then we must consider the practical range of variation of ϵ in the present circumstances. Whatever the absolute values of the local viscosities within the bilayer, the ratio $\eta_{head}/\eta_{midplane}$ is at least 50 (Venable et al., 1993). Our simple model implies that the cylinder height h must be smaller than the thickness of the hydrophobic core of the bilayer, i.e., smaller than 3 nm, as mentioned in the text. Thus the lowest limit of the a/h ratio is 0.2, the smallest value of a being 0.64 nm, as can be seen in Table 1. Consequently, the lower limit of ϵ is 25. The numerical solution carried out by Hughes et al. (1981) shows that the reduced drag coefficient $\Lambda(\epsilon)$ exhibits an asymptotic variation, provided that $\epsilon > 10$. Then $\Lambda(\epsilon) = 2/\pi$ is a reliable approximation and λ is simply given by $\lambda = 16a\eta_{head}$.

It was shown earlier that the same asymptotic solution applies to the study of the fluid mechanics of coexisting lipid monolayer domains (Klinger and McConnell, 1993). On the other hand, it is the limiting situation corresponding to the Saffman and Delbrück (1975) treatment that is relevant to the lateral diffusion of integral membrane proteins.

We are grateful to Pr. Marcin Majda (University of California, Berkeley) for very helpful discussions. UQ_8, UQ_5, UQ_4 and UQ_3 were a kind gift from EISAI Company LTD, Tokyo.

This work was supported in part by a grant from D.R.E.T. N° 95-159.

REFERENCES

Bain, C. D., J. Evall, and G. M. Whitesides. 1989. Formation of monolayers by the coadsorption of thiols on gold: variation in the head group, tail group and solvent. *J. Am. Chem. Soc.* 111:7155–7164.

Balcom, B. J., and N. O. Petersen. 1993. Lateral diffusion in model membranes is independent of the size of the hydrophobic region of molecules. *Biophys. J.* 65:630–637.

Bard, A. J., and L. R. Faulkner. 1980. Electrochemical Methods. John Wiley and Sons, New York.

Bassolino-Klimas, D., H. E. Alper, and T. R. Stouch. 1993. Solute diffusion in lipid bilayer membranes—an atomic level study by molecular dynamics simulation. *Biochemistry.* 32:12624–12637.

Bilewicz, R., and M. Majda. 1991. Monomolecular Langmuir-Blodgett films at electrodes. Formation of passivating monolayers and incorporation of electroactive reagents. *Langmuir.* 7:2794–2802.

Blackwell, M. F., K. Gounaris, S. J. Zara, and J. Barber. 1987. A method for estimating lateral diffusion coefficients of plastoquinone in membranes from steady state fluorescence quenching studies. *Biophys. J.* 51:735–744.

Blackwell, M. F., and J. Whitmarsh. 1990. Effect of integral membrane proteins on the lateral mobility of plastoquinone in phosphatidylcholine proteoliposomes. *Biophys. J.* 58:1259–1271.

Brian, A. A., and H. M. McConnell. 1984. Allogeneic stimulation of cytotoxic T cells by supported planar membranes. *Proc. Natl. Acad. Sci. USA.* 81:6159–6163.

Burke, L. D., D. T. Buckley, and J. A. Morrissey. 1994. Novel view of the electrochemistry of gold. *Analyst.* 119:841–845.

Castresana, J., A. Alonso, J-L. R. Arrondo, F. M. Goni, and H. Casal. 1992. The physical state of ubiquinone-10 in pure form and incorporated into phospholipid bilayers—a Fourier transform infrared spectroscopic study. *Eur. J. Biochem.* 204:1125–1130.

Charych, D. H., E. M. Landau, and M. Majda. 1991. Electrochemistry at the air water interface—lateral diffusion of an octadecylferrocene amphiphile in Langmuir monolayers. *J. Am. Chem. Soc.* 113:3340–3346.

Chazotte, B., and C. R. Hackenbrock. 1988. The multicollisional, obstructed, long-range diffusional nature of mitochondrial electron transport. *J. Biol. Chem.* 263:14359–14367.

Chazotte, B., and C. R. Hackenbrock. 1989. Lateral diffusion as a rate limiting step in ubiquinone mediated mitochondrial electron transport. *J. Biol. Chem.* 264:4978–4985.

Chazotte, B., E. S. Wu, and C. R. Hackenbrock. 1991. The mobility of a fluorescent ubiquinone in model lipid membranes—relevance to mitochondrial electron transport. *Biochim. Biophys. Acta.* 1058:400–409.

Cohen, M., and D. Turnbull. 1959. Molecular transport in liquids and glasses. *J. Phys. Chem.* 31:1161–1169.

Cornell, B. A., M. A. Kenery, A. Post, R. N. Robertson, L. E. Weir, and P. W. Westerman. 1987. Location and activity of ubiquinone-10 and analogues in model and biological membranes. *Biochemistry.* 26: 7702–7707.

Fato, R., M. Battino, M. Degli Espoti, G. Parenti Castelli, and G. Lenaz. 1986. Determination of partition and lateral diffusion coefficients of ubiquinones fluorescence quenching of *n*-(9-anthroyloxy)stearic acids in phospholipid vesicles and mitochondrial membranes. *Biochemistry.* 25: 3378–3790.

Fato, R., M. Battino, G. Parenti Castelli, and G. Lenaz. 1985. Measurement of the lateral diffusion coefficients of ubiquinones in lipid vesicles by fluorescence quenching of 12-(9-anthroyl)stearate. *FEBS Lett.* 179: 238–242.

Galla, H. J., W. Hartmann, U. Theilen, and E. Sackmann. 1979. On two dimensional passive random walk in lipid bilayers and fluid pathways in biomembranes. *J. Membr. Biol.* 48:215–236.

Gennis, R. B. 1989. Biomembranes: Molecular Structure and Function. Springer Verlag, New York.

Gordillo, G. J., and J. Schiffrin. 1994. Redox properties of ubiquinone adsorbed on a mercury electrode. *J. Chem. Soc. Faraday Trans.* 90: 1913–1922.

Gupte, S., E. S. Wu, L. Hoechli, M. Hoechli, K. Jacobson, A. E. Sowers, and C. R. Hackenbrock. 1984. Relationship between lateral diffusion, collision frequency and electron transfer of mitochondrial inner membrane oxidation-reduction components. *Proc. Natl. Acad. Sci. USA.* 81:2606–2610.

Handa, T., Y. Asai, K. Miyajima, Y. Kawashima, M. Kayano, K. Ida, and T. Ikeuchi. 1991. Relationship between lateral diffusion, collision frequency and electron transfer of mitochondrial inner membrane oxidation-reduction components. *J. Colloid Interface Sci.* 143:205–213.

Hauska, G., and E. Hurt. 1982. Pool function behavior and mobility of isoprenoid quinones. *In* Function of Quinones in Energy Conserving Systems. P. L. Trumpower, editor. Academic Press, New York. 87–110.

Heller, H., M. Schaefer, and K. Schulten. 1993. Molecular dynamics simulation of a bilayer of 200 lipids in the gel and in the liquid-crystal phases. *J. Phys. Chem.* 97:8343–8360.

Hughes, B. D., B. A. Pailthorpe, and L. R. White. 1981. The translational and rotational drag on a cylinder moving in a membrane. *J. Fluid Mech.* 110:349–372.

Johnson, M. E., D. A. Berk, D. Blankschtein, D. E. Golan, R. K. Jain, and R. S. Langer. 1996. Lateral diffusion of small compounds in human stratum corneum and model lipid bilayer systems. *Biophys. J.* 71: 2656–2668.

Kalb, E., S. Frey, and L. K. Tamm. 1992. Formation of supported planar bilayers by fusion of vesicles to supported phospholipid monolayers. *Biochim. Biophys. Acta.* 1103:307–312.

Klinger, J. F., and M. McConnell. 1993. Brownian motion and fluid mechanics of lipid monolayer domains. *J. Phys. Chem.* 97:6096–6100.

Lenaz, G., B. Samori, R. Fato, M. Battino, G. Castelli Parenti, and I. Domini. 1992. Localization and preferred orientations of ubiquinone homologs in model bilayers. *Biochem. Cell. Biol.* 70:504–514.

Marchal, D., W. Boireau, J-M. Laval, J. Moiroux, and C. Bourdillon. 1997. An electrochemical approach of the redox behavior of water insoluble ubiquinones and plastoquinones incorporated in supported phospholipid layers. *Biophys. J.* 72:2679–2688.

Metz, G., K. P. Howard, W. B. S. Vanliemt, J. H. Prestegard, J. Lugtenburg, and S. O. Smith. 1995. NMR studies of ubiquinone location in oriented model membranes: evidence for a single motionally averaged population. *J. Am. Chem. Soc.* 117:564–565.

Miller, C. J., and M. Majda. 1986. Microporous aluminum oxide films at electrodes. *J. Am. Chem. Soc.* 108:3118–3120.

Miller, C. J., C. A. Widrig, D. H. Charych, and M. Majda. 1988. Microporous aluminum oxide films at electrodes. 4. Lateral charge transport in self-organized bilayer assemblies. *J. Phys. Chem.* 92:1928–1936.

Millner, P. A., and J. Barber. 1984. Plastoquinone as a mobile redox carrier in the photosynthetic membrane. *FEBS Lett.* 169:1–6.

Mitchell, P., and J. Moyle. 1985. The role of ubiquinone and plastoquinone in chemiosmotic coupling between electron transfer and proton translocation. *In* Coenzyme Q. G. Lenaz, editor. John Wiley & Sons, New York. 12–19.

Parpaleix, T., J-M. Laval, M. Majda, and C. Bourdillon. 1992. Potentiometric and voltammetric investigations of H_2/H^+ catalysis by periplasmic hydrogenase from *Desulfovibrio gigas* immobilized at the electrode surface in an amphiphilic bilayer assembly. *Anal. Chem.* 64:641–646.

Pastor, R. W. 1994. Molecular dynamics and Monte Carlo simulations of lipid bilayers. *Curr. Opin. Struct. Biol.* 4:486–492.

Porter, M. D., T. B. Bright, D. L. Allara, and C. E. D. Chidsey. 1987. Spontaneously organized molecular assemblies. Structural characterization of alkyl thiol monolayers on gold by ellipsometry, infrared spectroscopy, and electrochemistry. *J. Am. Chem. Soc.* 109:3559–3568.

Rajarathnam, K., J. Hochman, M. Schindler, and S. Fergusson-Miller. 1989. Synthesis, location, and lateral mobility of fluorescently labeled ubiquinone 10 in mitochondrial and artificial membranes. *Biochemistry.* 28:3168–3176.

Rich, P. 1984. Electron and proton transfers through quinones and cytochrome bc complexes. *Biochim. Biophys. Acta.* 768:53–79.

Saffman, P. G., and M. Delbrück. 1975. Brownian motion in biological membranes. *Proc. Natl. Acad. Sci. USA.* 72:3111–3113.

Seelig, J., and A. Seelig. 1980. Lipid conformation in model membranes and biological membranes. *Q. Rev. Biophys.* 13:19–61.

Stidham, M., T. J. McIntosh, and J. Siedow. 1984. On the localization of ubiquinone in phosphatidylcholine bilayers. *Biochim. Biophys. Acta.* 767:423–431.

Tocanne, J. F., L. Dupoucezanne, and A. Lopez. 1994. Lateral diffusion of lipids in model and natural membranes. *Prog. Lipid Res.* 33:203–237.

Torchut, E., J-M. Laval, C. Bourdillon, and M. Majda. 1994. Electrochemical measurements of the lateral diffusion of electroactive amphiphiles in supported phospholipid monolayers. *Biophys. J.* 66:753–762.

Tscharner, V. V., and H. M. McConnell. 1981. Physical properties of lipid monolayers on alkylated planar glass surfaces. *Biophys. J.* 36:421–427.

Ulrich, E. L., M. E. Girvin, W. A. Cramer, and J. L. Markley. 1985. Location and mobility of ubiquinones of different chain lengths in artificial membrane vesicles. *Biochemistry.* 24:2501–2508.

Vaz, W. L. C., R. M. Clegg, and D. Hallmann. 1985. Translational diffusion of lipids in liquid crystalline phase phosphatidylcholine multibilayers. A comparison of experiment with theory. *Biochemistry.* 24:781–786.

Vaz, W. L. C., F. Goodsaid-Zalduondo, and K. Jacobson. 1984. Lateral diffusion of lipids and proteins in bilayer membranes. *FEBS Lett.* 174: 199–210.

Venable, R. M., Y. Zhang, B. J. Hardy, and R. W. Pastor. 1993. Molecular dynamics simulations of a lipid bilayer and of hexadecane. An investigation of membrane fluidity. *Science.* 262:223–226.

Volkenstein, V. M. 1963. High Polymers No. 17. Interscience Publishers, John Wiley and Sons, New York.

Wilson, M. A., and A. Pohorille. 1994. Molecular dynamics of a water-lipid bilayer interface. *J. Am. Chem. Soc.* 116:1490–1501.